Reference: *Biol. Bull.* **205:** 36–46. (August 2003)

Twisting and Bending of Biological Beams: Distribution of Biological Beams in a Stiffness Mechanospace

SHELLEY A. ETNIER*

Department of Biology, Duke University, Durham, North Carolina 27708-0338

Abstract. Most biological beams bend and twist relatively easily compared to human-made structures. This paper investigates flexibility in 57 diverse biological beams in an effort to identify common patterns in the relationship between flexural stiffness and torsional stiffness. The patterns are investigated by mapping both ideal and biological beams into a mechanospace defined by flexural and torsional stiffness. The distribution of biological beams is not random, but is generally limited to particular regions of the mechanospace. Biological beams that are stiff in bending are stiff in torsion, while those that bend easily also twist easily. Unoccupied regions of the mechanospace represent rare combinations of mechanical properties, without proving that they are impossible. The mechanical properties of biological beams closely resemble theoretical expectations for ideal beams. Both distributions are potentially being driven by the interdependence of the material and structural properties determining stiffness. The mechanospace can be used as a broadly comparative tool to highlight systems that fall outside the general pattern observed in this study. These outlying beams may be of particular interest to both biologists and engineers due to either material or structural innovations.

Introduction

Flexibility, or the ability to deform in response to a load, is a property of most biological beams (Vogel, 1984; Denny, 1988), yet the biological consequences of flexibility vary widely. In motile organisms, flexibility permits the relative movements of structural elements in response to internal forces generated by muscular contractions or hydrostatic pressures. The flexibility of a fish backbone influences the mechanical behavior of the body during undulatory swimming (McHenry *et al.*, 1995; Long and Nipper, 1996), while the flexibility of mammalian backbones has been implicated in locomotor differences between species (Gàl, 1993). In many sessile organisms, flexibility allows structures to passively adjust their posture relative to the forces experienced (Wainwright *et al.*, 1976; Vogel, 1984). Leaf petioles (Vogel, 1989; Niklas, 1991) and herbaceous plants (Ennos, 1993; Etnier and Vogel, 2000) reduce flow-induced drag by bending or twisting in response to wind, and similar drag-reducing mechanisms have been found in hydroid colonies (Harvell and LaBarbera, 1985) and anemones (Koehl, 1977a). Other flexible organisms take advantage of external forces to passively orient their filter-feeding structures in response to ever-changing flow (Wainwright and Dillon, 1969; Koehl, 1977b; Harvell and LaBarbera, 1985; Best, 1988). Thus, the ability to deform in response to loads is observed in both motile and sessile organisms living in either an aquatic or a terrestrial environment, apparently independent of phylogenetic affiliations. Such convergence may be viewed as a red flag indicating the tremendous importance of flexibility in the design of biological organisms (Lauder, 1982; Vogel, 1998).

Flexibility is measured in terms of stiffness, where flexural stiffness (EI in $N \cdot m^2$) represents the resistance of a beam (a structure that is long relative to its width) to bending, and torsional stiffness (GJ in $N \cdot m^2$) represents the resistance of a beam to twisting. Flexural stiffness and torsional stiffness are composite variables that are influenced both by material and structural properties (Wainwright *et al.*, 1976). Every beam is characterized by a combination of flexural stiffness and torsional stiffness, and the relationship between these two variables determines

Received 14 February 2003; accepted 21 May 2003.

*Present address: University of North Carolina at Wilmington, 601 S. College Road, Wilmington, NC 28403. E-mail: etniers@uncwil.edu

how the beam responds to a given load. The ratio of flexural stiffness to torsional stiffness, commonly termed the twist-to-bend ratio, has been used as a dimensionless (and, thus, size invariant) index describing the relationship between these two variables (Niklas, 1992; Vogel, 1992, 1995; Etnier and Vogel, 2000). The twist-to-bend ratio indicates the relative resistance of a beam to bending *versus* twisting. More intuitively, a higher twist-to-bend ratio indicates a structure that twists more readily than it bends, without reference to the magnitude of either variable.

While flexibility is a common property of a phylogenetically diverse group of organisms, are there any common patterns or trends in the relationship between flexural stiffness and torsional stiffness in biological beams? This paper investigates such patterns with a mechanospace defined by values of flexural and torsional stiffness. The mechanospace, similar to Raup's (1966) classic morphospace, is a broadly comparative tool used to visualize the relationships between mechanical variables in biological beams. The concept is based on the premise that the mechanical properties of flexural and torsional stiffness are common to all biological beams. Three variations of this mechanospace will be used to compare the patterns of flexibility seen in a large diversity of biological structures. First, material and structural properties will be used in combination to predict, on the basis of principles of engineering beam theory, the theoretical relationships between bending and twisting in ideal beams. Second, experimentally measured values of flexural stiffness and torsional stiffness for biological structures will be examined within the context of the theoretical distribution. Finally, the relative contribution of overall size to the mechanical properties of biological beams will be explored. The results suggest that the distribution of biological beams within the mechanospace is not random, due to the interdependence of material and structural properties determining stiffness.

Materials and Methods

Distribution of ideal beams

The distribution of ideal beams was determined using principles from engineering beam theory. Importantly, this distribution is limited to structures built of a single, isotropic material (*i.e.*, the material properties are not directionally variable), with precise specifications for the cross-sectional shape of the beam in question (Roark, 1943). Additionally, engineering beam theory stipulates that the material is linearly elastic, and that the beam is straight and does not vary in size or shape along its length, nor does the beam undergo deflections greater than 10% of total length (Roark, 1943). More complex solutions are required for beams that undergo larger deflections (*e.g.*, Morgan and Cannell, 1987; Morgan, 1989).

Material properties. The material properties influencing flexural stiffness and torsional stiffness are Young's modulus (E in $N \cdot m^{-2}$) and the shear modulus (G in $N \cdot m^{-2}$), respectively. Young's modulus and the shear modulus are related to one another by Poisson's ratio (ν), which is the dimensionless ratio of the induced strain, causing lateral contraction of the specimen, to the applied strain, causing the specimen to elongate (Vincent, 1990). Poisson's ratios can vary from 0 to 0.50 for naturally occurring isotropic materials. Mollusc shell has a Poisson's ratio of about 0.10, while rubber has a ratio closer to 0.50 (Denny, 1988) and materials such as cornstalks have moderate ratios around 0.23 (Prince and Bradway, 1969). Commonly occurring metals have Poisson's ratios between 0.25 and 0.30 (Niklas, 1992).

For isotropic materials, the shear modulus is related to Young's modulus (Roark, 1943) by:

$$G = \frac{E}{2(1 + \nu)} \tag{1}$$

Thus, the Young's modulus for a typical isotropic material will range from 2 to 3 times its shear modulus as Poisson's ratio varies from 0 to 0.50 (Wainwright *et al.*, 1976; Niklas, 1992).

Structural properties. The structural variables influencing flexural stiffness and torsional stiffness are the second moment of area (I in m^4) and the polar moment of area (J in m^4), respectively. These variables reflect the geometry of a cross section of a beam and are influenced by size, shape, and orientation (Roark, 1943). The relationship between I and J depends upon the cross-sectional shape of the structure in question (Roark, 1943). Formulas for the calculation of I and J for most simple shapes can be found in any basic engineering handbook (*e.g.*, Gere and Timoshenko, 1984). I and J are both proportional to radius to the fourth power, hence radius is a very strong determinant of stiffness (Roark, 1943). For example, for a beam with a circular cross-sectional area

$$I = \frac{\pi r^4}{4} \quad \text{and} \quad J = \frac{\pi r^4}{2} \tag{2}$$

the value of I/J is 0.50. Small changes in the cross-sectional shape of a beam can greatly influence the values of I and J; thus, the value I/J for noncircular cross sections can be much higher (Table 1). Note that there may be several values of I/J for a beam with an asymmetric cross-sectional shape, depending on its orientation with respect to the applied load (Table 1).

Relationship between flexural and torsional stiffness. EI and GJ are dependent variables, with Poisson's ratio linking the material properties (E and G), and geometry linking the structural properties (I and J). Theoretically, the relationship between flexural stiffness and torsional stiff-

Table 1

Theoretical relationships between flexural and torsional stiffness

Cross-sectional shape		*I*/*J*	Ratio of *EI*/*GJ*	
			If $\nu = 0$, then $E/G = 2$	If $\nu = 0.50$, then $E/G = 3$
Circle		0.50	1.00	1.50
Ellipse 4:1 major:minor axis		0.27	0.54	0.81
Ellipse 4:1 major:minor axis		4.25	8.50	12.75

The ratio of *I*/*J* was determined from beam-theory equations (Niklas, 1992) and represents the structural contributions to stiffness in these beams. For the ellipses, *I* is calculated about the axis indicated by the dashed line. The ratio of *E*/*G* represents the material contribution to beam stiffness as Poisson's ratio was allowed to vary from 0 to 0.50. The chosen cross-sectional shapes are broadly representative of biological beams (Wainwright, 1988).

ness can vary only slightly, based on this interdependence. The relationships between flexural stiffness and torsional stiffness can be calculated for beams of different shapes and materials (Table 1). The ratio of *EI*/*GJ* for a given circular beam can range between 1 and 1.5 as Poisson's ratio varies from 0 to 0.5. In contrast, an elliptical beam with a major to minor axis ratio of 4.1 has a range of *EI*/*GJ* (with *EI* measured about the minor axis) from 8.50 to 12.75 for the same range in Poisson's ratio (Niklas, 1992). These particular cross-sectional shapes are presented because they are broadly representative of biological beams (Wainwright, 1988). Note that two beams can have the same *EI*/*GJ* ratio despite vast differences in size, shape, and material because the ratio is determined by the relative magnitudes of flexural stiffness to torsional stiffness, not by their absolute values.

The relationship between *EI* and *GJ* for ideal beams can be mapped into a mechanospace defined by these variables (Fig. 1). Each quadrant of the mechanospace represents different combinations of flexural stiffness and torsional stiffness, ranging from the upper left, where beams twist easily but do not bend, to the lower right, where beams bend easily but do not twist. The dashed line in Figure 1 represents a circular beam with a moderate Poisson's ratio of 0.25. The solid lines in Figure 1 represent the two orientations of a beam with a 4:1 elliptical cross-sectional shape as Poisson's ratio is maximized ($\nu = 0.5$) or minimized ($\nu = 0$). An elliptical beam of this form was chosen because such an ellipse has a large *I*/*J* ratio and likely represents an extreme shape for biological structures. Thus, the area between the two solid lines represents the range of values for beams with moderate to extreme material values, with shapes that are broadly representative of biological beams (Wainwright, 1988). Importantly, the solid lines do not represent absolute theoretical limits, but rather identify the expected extremes for ideal beams composed of a single, isotropic material. Greater shape modification will slightly alter these limits.

Distribution of biological beams

Although biological beams are commonly modeled using beam theory (*e.g.*, Koehl, 1977b; Carrier, 1983; Vogel, 1992; Baumiller, 1993; Ennos, 1993; Vogel, 1995; Niklas, 1998; Etnier and Vogel, 2000; Etnier, 2001), they are rarely, if ever, made up of a single, isotropic material. More typically, they are made up of multiple materials, whose distribution varies both across the cross section of the beam and along its length. Yet, in practice, flexural stiffness and torsional stiffness are measured experimentally using basic engineering formulas for beams. In general, a known load is applied to a beam, causing it to deform, either by bending or by twisting. The exact equation used is dependent on how the beam is loaded. For example, for end-loaded cantilever beams (one end fixed and the other end free to deform), flexural stiffness is calculated as:

$$EI = \frac{FL^3}{3y} \tag{3}$$

where F is the applied force, L is the length of the specimen, and y is the deflection of the free end of the specimen (Gere and Timoshenko, 1984). Similarly, torsional stiffness is calculated using the following formula:

$$GJ = \frac{Fd}{\theta/L} \tag{4}$$

where F is the force applied at a moment arm d, L is the length of the specimen, and θ is the rotation of the free end in radians (Gere and Timoshenko, 1984).

Data were compiled from the literature and from the

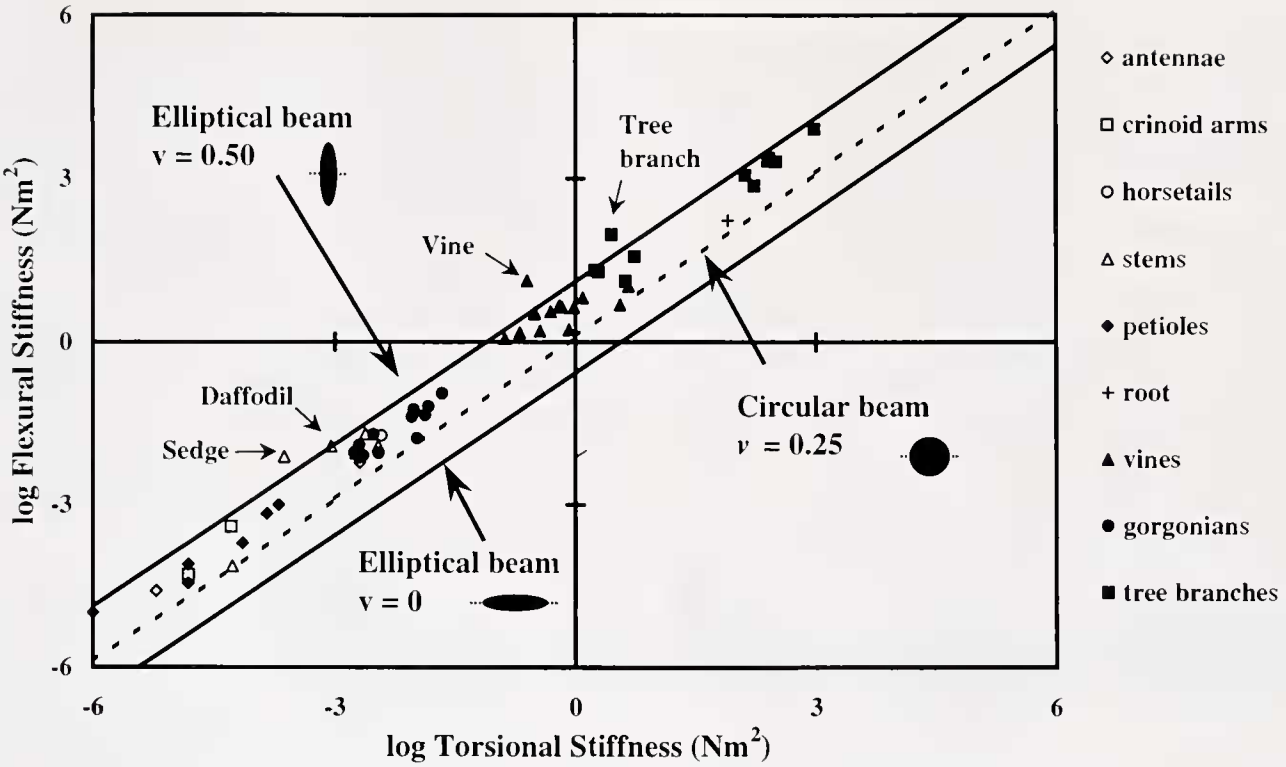

Figure 1. The mechanospace defined by values of flexural stiffness and torsional stiffness. The lines represent the distribution of ideal beams based upon an assumed cross-sectional shape and Poisson's ratio. The symbols represent the nine groups (Table 2), with each individual point representing an average value for a species (appendix). The upper line represents an elliptical beam (4:1 major to minor axis) with *I*/*J* calculated about the short axis and a Poisson's ratio of $\nu = 0.50$. The lower line represents that same beam with *I*/*J* calculated about the long axis and a Poisson's ratio of $\nu = 0$. The dashed line represents a circular beam with a Poisson's ratio of $\nu = 0.25$.

author's research to obtain average flexural stiffness and torsional stiffness measures for 25 species of plants and animals (see appendix). These data were obtained following protocols similar to those discussed above. In other cases ($n = 32$), published data consisted only of measures of *E* and *G*. In these cases, the researchers experimentally determined *EI* and *GJ*, but then factored out *I* and *J* based on the cross-sectional size and shape of the structures. But note that the experimental data were still based on the overall mechanical behavior of the beam (*i.e.*, deformation due to a load), rather than direct measures of material properties. In cases where published data consisted only of measures of *E* and *G*, both size and shape were estimated to determine values for *I* and *J* (appendix). Flexural stiffness and torsional stiffness were then calculated, based on these estimates. The estimates of beam diameter were deliberately conservative, while cross-sectional shape was always assumed to be circular. For example, for 14 of the 16 vines and 5 of the 11 tree branches included in the mechanospace, the beam was assumed to have a circular cross section with a diameter of 0.02 m. The reported diameters for these species were 0.02–0.05 m (Putz and Holbrook, 1991). Similar assumptions were made for the gorgonian corals, with an estimated diameter of 0.002 m (Jeyasuria and Lewis, 1987). The assumption of a relatively small diameter will affect the overall magnitudes of flexural stiffness and torsional stiffness, but will not affect the ratio of the two. The assumption of a circular cross-sectional shape will result in lower estimated values of *I*/*J* than would be seen in noncircular beams (Table 1).

The species (total $n = 57$) were divided into nine groups based upon broad morphological similarities (Table 2). Structures varied greatly in size, with diameters ranging from 0.001 m (red maple petioles) to 0.05 m (small tree branches). Average values for log *GJ versus* log *EI* for all species ($n = 57$) were plotted in the mechanospace (Fig. 1). Note that each point represents an average value for a species, and thus does not reflect individual variation in size and material properties. For asymmetric beams, such as the daffodils, crinoid arms, and crustacean antennae, flexural stiffness is reported as the average of the different orientations. Coefficients of variation for these organisms varied between 35% and 196% for flexural stiffness, and from 36% to 110% for torsional stiffness (Etnier and Vogel, 2000;

Table 2

Basic group characteristics for beams analyzed in this study

Groups	Basic characteristics
Crustacean antennae	Multi-jointed beam. Antennae used for sensory information and in some cases, for aggressive interactions. Not loaded gravitationally. Aquatic animal.
Crinoid arms	Multi-jointed beam. Arms used for passive filter feeding. Not loaded gravitationally. Aquatic animal.
Horsetails	Multi-jointed beam. Stem must maintain upright position for photosynthesis, so self-supporting. Terrestrial plant.
Herbaceous stems	Continuous beam. Stem must maintain upright position for photosynthesis, so self-supporting. Terrestrial plant.
Leaf petioles	Continuous beam. Petiole must support leaf against gravity and withstand wind, so self-supporting. Terrestrial plant.
Tree roots	Continuous beam. Root is not self-supporting. Loaded in tension. Terrestrial plant.
Vines	Continuous beam. Vine is not self-supporting. Loaded in tension. Terrestrial plant.
Gorgonian corals	Continuous beam. Support individual polyps against water flow. Not loaded gravitationally. Aquatic animal.
Tree branches	Continuous beam. Tree must maintain upright position for photosynthesis, so self-supporting. Terrestrial plant.

The biological beams investigated were divided into nine groups, based on broad differences in morphology and function.

Etnier, 2001), reflecting the individual variation noted above.

The twist-to-bend ratio for each species was calculated and compared to the predicted values as an additional descriptor of flexibility in biological beams (Fig. 2). Standard deviations for the twist-to-bend ratios, when available, are reported in the appendix.

Size-normalized mechanospace

Size greatly influences the stiffness of a biological beam, both in twisting and in bending. The structural variables, I and J, are both proportional to radius to the fourth power; thus, small increases in size will greatly increase beam stiffness, regardless of cross-sectional shape or material composition. Values of EI and GJ were normalized for size by dividing by radius to the fourth power to determine if size alone was driving the observed patterns. These values were then mapped into a size-normalized mechanospace (Fig. 3). This normalization accounts for size alone, rather than equating to calculations of E or G for a given beam.

Results

The lines shown in Figure 1 are based upon the assumptions of engineering beam theory and represent values for ideal beams. The distribution of biological beams closely matched that of the ideal beams, with 93% (53 of 57) of the points falling within the bounded region (Fig. 1). The boundaries reflect possible extremes for biological beams, based on assumed material values and chosen cross-sectional shapes. Flexural stiffness and torsional stiffness changed concurrently in the biological beams. Thus, beams that bent easily also twisted easily, while those that were hard to bend were also hard to twist. Overall, flexural stiffness and torsional stiffness each varied over 9 orders of magnitude. Species within the defined groups occupied similar regions of the mechanospace, implying that the flexural stiffness and torsional stiffness of group members were of similar magnitude.

Due to the finite nature of the data set, the unoccupied regions of the mechanospace suggest that other combinations of mechanical values are rare without proving that they are impossible. Biological beams may exist within these unoccupied regions, given sufficient variation in material or structural design. The four samples falling outside of the predicted boundaries for ideal circular and elliptical beams included two herbaceous stems (daffodils *Narcissus pseudonarcissus* and sedges *Carex acutiformis*), a tree branch (*Dendropanex arboreus*), and a tropical vine (*Marcgravia rectiflora*). These systems were all characterized by high flexural stiffness relative to torsional stiffness—that is, they twisted more easily than they bent (Fig. 2).

Twist-to-bend ratios varied dramatically among different species (Fig. 2), with both the maximum (52.9) and the minimum (1.4) occurring in tropical vines. The average twist-to-bend ratio for all groups combined was 7.2, which falls between the predicted values for ideal beams that are circular or elliptical in cross-sectional shape.

When the data were normalized for size (Fig. 3), the observed distribution changed slightly. In particular, the relative position of the antennae, horsetail rushes, and gorgonian corals shifted up and to the right relative to the other beams. This result suggests that these structures are all relatively stiff for their size. While the position of groups changed slightly, structures that were stiffer in bending were also stiffer in torsion, regardless of their overall size.

Discussion

The close resemblance in the distribution of ideal and biological beams suggests that both are limited by the interdependence between the material properties, E and G, and between the geometric properties, I and J. Yet, keep in mind the assumptions of beam theory, which are violated almost universally by biological beams. The theoretical relationships apply only to beams consisting of a single,

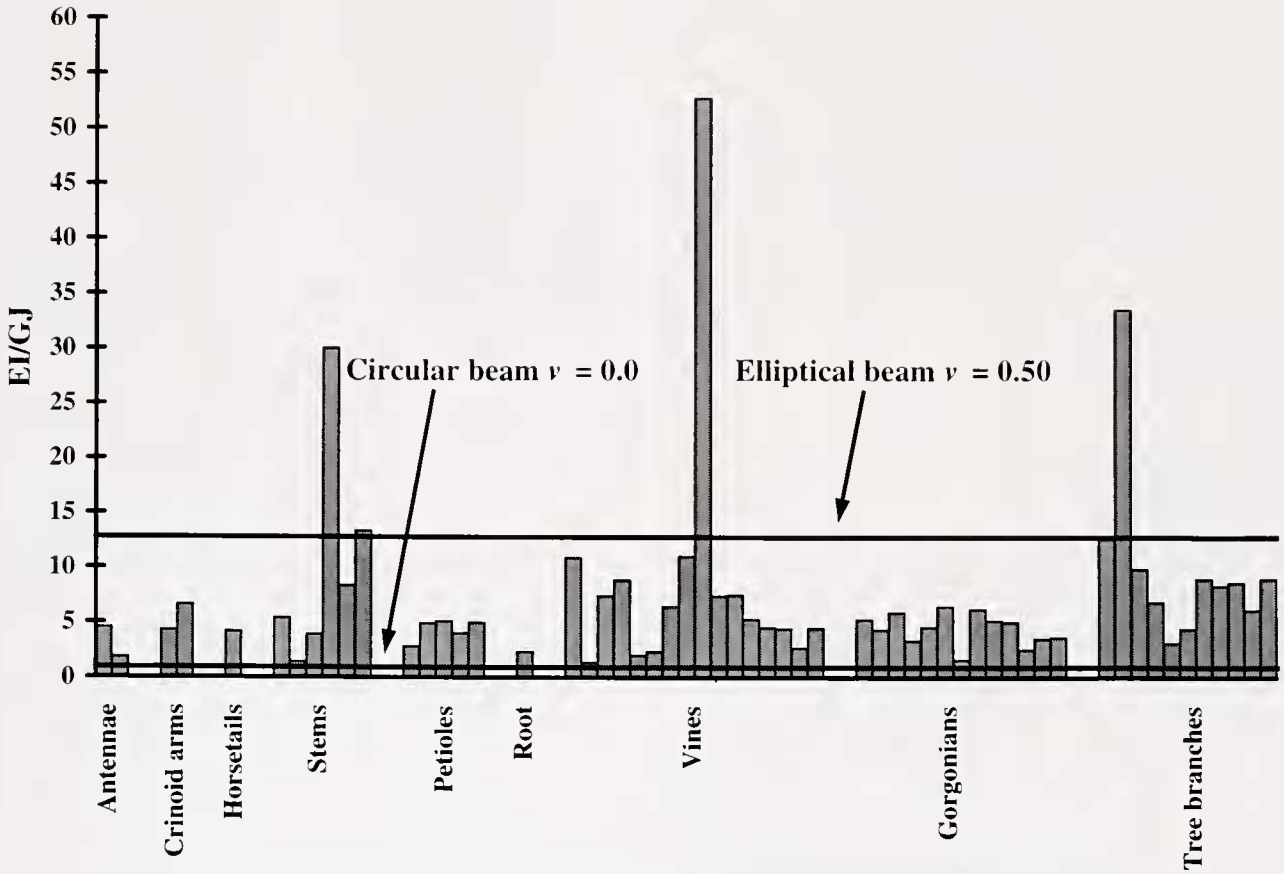

Figure 2. Twist-to-bend ratios for the nine groups. The horizontal lines indicate the predicted values for ideal beams with circular ($EI/GJ = 1.00$, $\nu = 0$) and elliptical ($EI/GJ = 12.75$, $\nu = 0.50$) cross sections. The beams are arranged by size within each group, with the smallest diameter beam to the left. Standard deviations for the twist-to-bend ratios, when available, are reported in the appendix.

isotropic material (Roark, 1943). Biological materials are more typically anisotropic, and values for Poisson's ratio can vary greatly from the theoretical expectations (Vincent, 1990). More importantly, biological beams are almost always composite structures built of multiple materials that differ greatly in their mechanical properties. Thus, it is not obvious that *EI* and *GJ* would be highly interdependent in biological beams, particularly in the beams that deviate most from the theoretical assumptions, such as the jointed crinoid arms or crustacean antennae.

The four samples falling outside of the predicted boundaries are all characterized by high flexural stiffness relative to torsional stiffness—that is, they will twist more easily than bend (Fig. 2). The two herbaceous stems have flowers or seed heads that extend perpendicular to the long axis of the stem, potentially causing the stem to bend or twist when the wind blows. Rather than resisting this load with a high torsional stiffness, daffodils (*Narcissus pseudonarcissus*) and sedges (*Carex acutiformis*) have a low torsional stiffness, which allows them to twist in the wind. Daffodils reduce flow-induced drag with this action (Etnier and Vogel, 2000), and a similar function has been suggested for sedges (Ennos, 1993). The functional relevance of the high ratios of flexural stiffness to torsional stiffness in the tree trunk and vine has not been explored.

Conservative estimates of size and shape were made for many of the tree branches, vines, and gorgonian corals (appendix). Beam size affects *EI* and *GJ* equally; thus, errors in the size estimates will not affect the position of data points relative to the predicted boundaries (Fig. 4). Rather, an increase or decrease in diameter will cause these points to shift parallel to the boundaries. In contrast, shape estimates will differentially affect *EI* and *GJ*, causing data points to shift relative to the predicted boundaries (Fig. 4). Although branches and vines are fairly circular in cross section, this assumption may not be valid for the gorgonian corals, whose cross-sectional shape can be circular, elliptical, or even triangular (Jeyasuria and Lewis, 1987). The assumption of a circular cross section potentially underestimates the range of values seen in the gorgonian corals. For example, if the cross-sectional shape of the gorgonians is assumed to be a 4:1 ellipse rather than circular, then all of

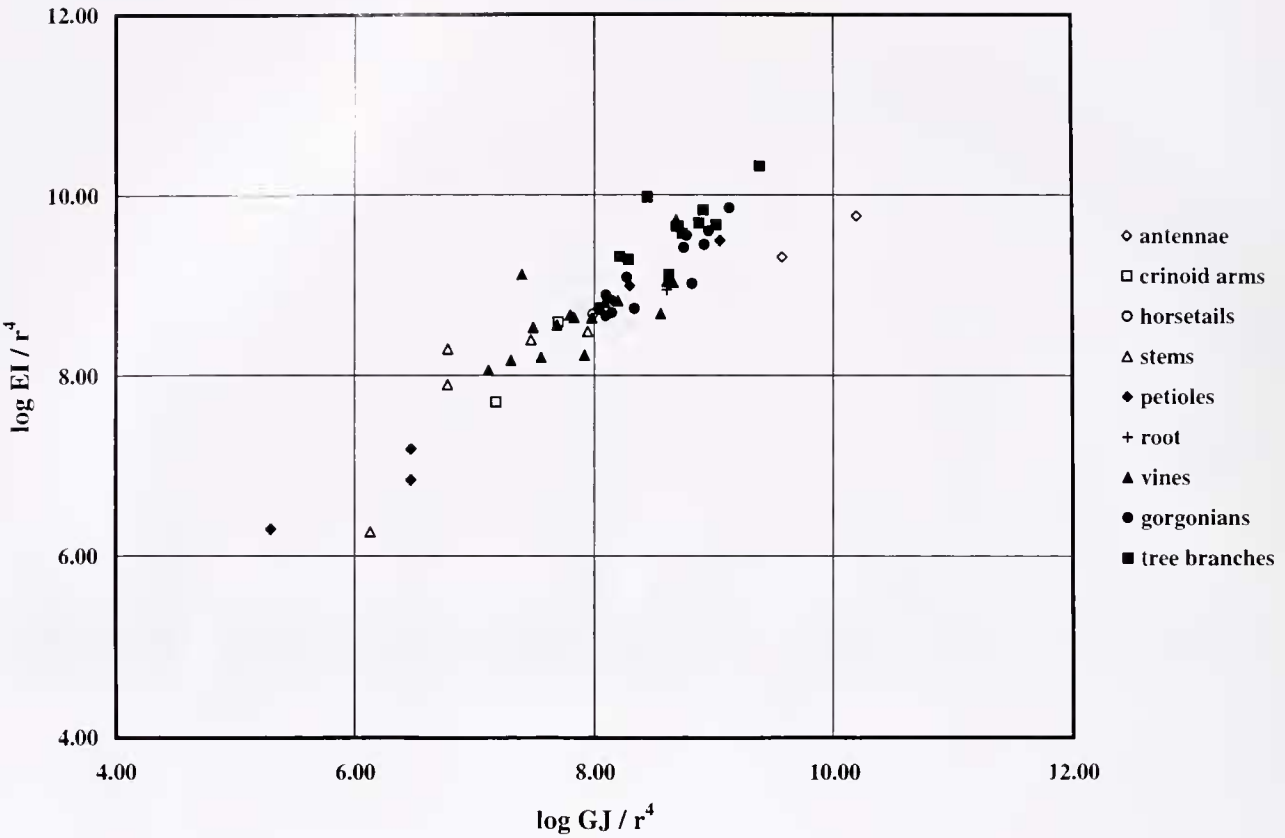

Figure 3. Flexural and torsional stiffness normalized by size for all groups (Table 2). The data points were normalized by dividing by radius to the fourth power.

these beams will fall outside of the predicted boundaries. Future studies that include the cross-sectional shape of the gorgonian corals may identify group members that are of particular mechanical and functional interest within a biological context.

Flexural stiffness and torsional stiffness are both highly dependent on the size of the structure in question. While the pattern seen in the stiffness mechanospace is driven in part by size increases alone, the size-normalized mechanospace (Fig. 3) suggests a robust pattern. Even with differences in size removed from the comparison, there is still a strong relationship between how a beam bends and how it twists. The size-normalized mechanospace suggests some interesting comparisons between the different groups. For example, the antennae have a size-normalized flexural stiffness similar to that of tree branches, while exhibiting a higher size-normalized torsional stiffness. Again, the biological implications of such variation have not been sufficiently explored in the literature.

The size, shape, and function of a beam may change during development (Wainwright and Dillon, 1969; Carrier, 1983; Katz and Gosline, 1992; Gallenmüller *et al.*, 2001). Such changes potentially influence both flexural stiffness and torsional stiffness, thus affecting how the beam responds to a given load. The mechanospace introduced in this study is well suited for investigations relating the morphology, mechanics, and functional demands of biological beams during ontogeny. A systematic study of the relationship between *EI* and *GJ* over a developmental series can reveal clues to the changing functional demands on a system during growth (Gallenmüller *et al.*, 2001). Concurrent morphological studies could determine whether mechanical changes are due to variation in material or structural properties, potentially identifying the mechanisms that different systems use to modulate mechanical properties.

Species within a group occupy a similar region of the mechanospace, signifying that the flexural stiffness and torsional stiffness of group members are of similar magnitude. The same pattern is true for the size-normalized mechanospace. While group members tend to occupy similar regions of the mechanospace, there is still variation within each group. Interspecific variation in shape and material may permit different combinations of flexural and torsional stiffness that may subtly influence how each species functions in its environment.

Despite clear differences in design, no obvious mechanical differences distinguish jointed beams from continuous beams. In continuous biological beams, the observed me-

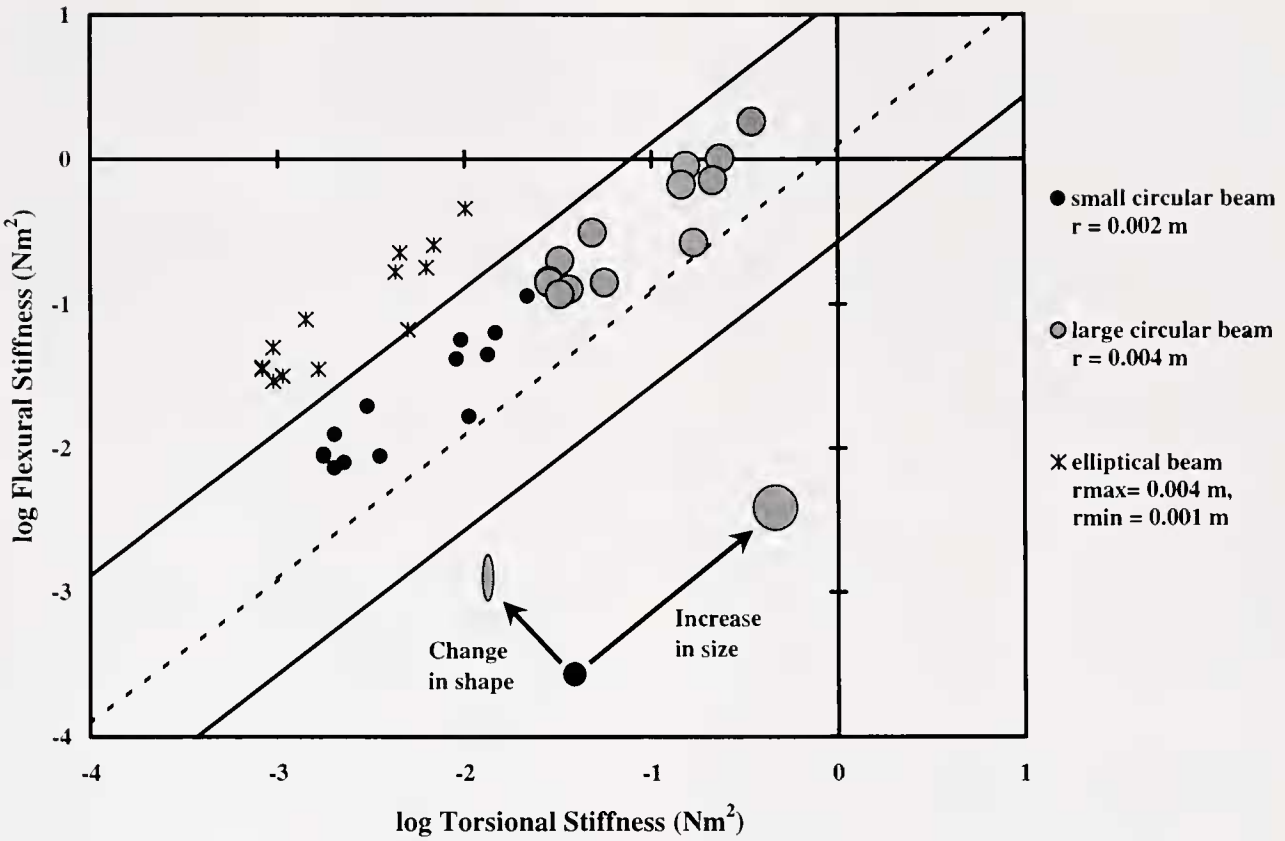

Figure 4. Changes in the assumptions of size and shape of beams will affect their distribution in the mechanospace. The small filled circles are the gorgonian values graphed in Figure 1 and were based on an assumed radius of 0.002 m. The lines represent the predicted values for ideal beams discussed previously. Changes in radius will affect the magnitude of I and J equally; thus, an increase or decrease in radius will cause these points to shift parallel to the predictions. For example, increasing the radius from $r = 0.002$ m to $r = 0.004$ m shifts the distribution up and to the right (large circles). In contrast, shape estimates differentially affect I and J. If the cross-sectional shape is assumed to be a 4:1 ellipse ($r_{max} = 0.004$ m, $r_{min} = 0.001$ m) rather than a circle, and I is calculated about the short axis, the data points move outside of the upper boundary (stars). Note that the cross-sectional area of the elliptical beams is equivalent to that of the small, circular beams; thus, these changes do not reflect an increase in the total amount of material, but rather a change in its distribution.

chanical properties may be attributed to materials that extend the entire length of the beam, but this explanation is inadequate for the jointed beams, which have no materials extending uninterruptedly along their entire length. The similarity in values for flexural stiffness and torsional stiffness for both jointed and continuous systems suggests that these beams may represent alternative designs to meet the functional need for flexibility in biological structures. Two of the jointed systems, horsetails and antennae, are relatively stiff for their size, suggesting that the presence of joints does not necessarily equate with increased flexibility.

Neither the ideal beams nor the biological beams are distributed uniformly throughout the mechanospace (Fig. 1). Unoccupied regions of the mechanospace correspond to beams that bend but do not twist and beams that twist but do not bend. The distribution within the mechanospace may be determined by inherent principles governing the relationships between E and I, as well as G and J. Conversely, empty areas within the distribution may not be an indication of physical impossibility, but of evolutionary history. There may be an absence of environmental patterns of change causing natural selection for particular combinations of mechanical properties (Raup and Stanley, 1971). Alternatively, once an evolutionary pathway has been initiated, phylogenetic canalization may limit future options for change (Lauder, 1982). Finally, empty spaces within the mechanospace may reflect temporal, rather than physical, limitations to those areas (Raup, 1966). The empty spaces will eventually be occupied, given enough time. Although the identification of boundaries within this mechanospace may not reveal their ultimate source, the boundaries do identify factors that may influence the observed pattern (Lessa and Patton, 1989).

Despite the structural diversity of the samples used in this study, they are merely a subset of the biological possibilities. A notable limitation is the absence of fiber-wrapped beams in the mechanospace. Internally pressurized, hydrostatic skeletons are typically wrapped with reinforcing fibers (Wainwright *et al.*, 1978). The fibers may be arranged orthogonally with the fibers parallel and perpendicular to the long axis of the structure, or they may be in a helical array with fibers running in right- and left-handed helices around the long axis. Orthogonal arrays offer little resistance to twisting, while being relatively stiff in bending (Wainwright *et al.*, 1978). Thus, these beams would potentially fall into the upper left-hand corner of the mechanospace. In contrast, helical fiber arrays allow pressurized beams to bend smoothly without kinking, while resisting torsional deformations (Wainwright *et al.*, 1978), potentially positioning these beams in the lower right of the mechanospace. Fibrous support systems may decouple the relationship between *EI* and *GJ*, permitting novel combinations of mechanical properties. Thus, their inclusion in the mechanospace may greatly expand the observed distribution.

The mechanospace presented here is a useful approach for investigating patterns of flexibility in biological beams. Importantly, the mechanospace does not imply that flexibility has critical functional relevance in each system. Rather, it should be used as a broadly comparative tool to highlight systems in which flexibility may be biologically important. Biological beams that do not follow the basic pattern seen in the mechanospace may be of particular interest to both biologists and engineers, either due to material or structural innovation.

Acknowledgments

I am grateful for the comments of Dr. Steve Vogel, Dr. Steve Wainwright, and Dr. Bill Hoese on early drafts of this manuscript, as well as informative and invaluable discussions with Dr. John Gosline and Dr. D. A. Pabst. This manuscript was greatly improved by the comments of the reviewers.

Literature Cited

Baumiller, T. K. 1993. Crinoid stalks as cantilever beams and the nature of the stalk ligament. *Neues Jahrb. Geol. Palaeontol. Abh.* **190:** 279–297.

Best, B. A. 1988. Passive suspension feeding in a sea pen: effects of ambient flow on volume flow rate and filtering efficiency. *Biol. Bull.* **175:** 332–342.

Carrier, D. R. 1983. Postnatal ontogeny of the musculo-skeletal system in the black-tailed jack rabbit (*Lepus californicus*). *J. Zool.* **201:** 27–55.

Denny, M. W. 1988. *Biology and the Mechanics of the Wave-swept Environment.* Princeton University Press, Princeton, NJ.

Ennos, A. R. 1993. The mechanics of the flower stem of the sedge *Carex acutiformis*. *Ann. Bot.* **72:** 123–127.

Etnier, S. A. 1999. Flexural and torsional stiffness in biological beams: the morphology and mechanics of multi-jointed structures. Ph.D. dissertation. Duke University, Durham, NC. 147 pp.

Etnier, S. A. 2001. Flexural and torsional stiffness in multi-jointed biological beams. *Biol. Bull.* **200:** 1–8.

Etnier, S. A., and S. Vogel. 2000. Reorientation of daffodil (*Narcissus*: Amaryllidaceae) flowers in wind: drag reduction and torsional flexibility. *Am. J. Bot.* **87:** 29–32.

Gál, J. 1993. Mammalian spinal biomechanics. II. Intervertebral lesion experiments and mechanisms of bending resistance. *J. Exp. Biol.* **174:** 281–297.

Gallenmüller, F., U. Miller, N. Rowe, and T. Speck. 2001. The growth form of *Croton pullei* (Euphorbiaceae)—functional morphology and biomechanics of a neotropical liana. *Plant Biol.* **3:** 50–61.

Gere, J. M., and S. P. Timoshenko. 1984. *Mechanics of Materials.* Brooks/Cole Engineering Division, Monterey, CA.

Harvell, C. D., and M. LaBarbera. 1985. Flexibility: a mechanism for control of local velocities in hydroid colonies. *Biol. Bull.* **168:** 312–320.

Jeyasuria, P., and J. C. Lewis. 1987. Mechanical properties of the axial skeleton in gorgonians. *Coral Reefs* **5:** 213–219.

Katz, S. L., and J. M. Gosline. 1992. Ontogenetic scaling and mechanical behaviour of the tibiae of the African desert locust (*Schistocerca gregaria*). *J. Exp. Biol.* **168:** 125–150.

Koehl, M. A. R. 1977a. Effects of sea anemones on the flow forces they encounter. *J. Exp. Biol.* **69:** 87–105.

Koehl, M. A. R. 1977b. Mechanical organization of cantilever-like sessile organisms: sea anemones. *J. Exp. Biol.* **69:** 127–142.

Lauder, G. V. 1982. Historical biology and the problem of design. *J. Theor. Biol.* **97:** 57–67.

Lessa, E. P., and J. L. Patton. 1989. Structural constraints, recurrent shapes and allometry in pocket gophers genus *Thomomys*. *Biol. J. Linn. Soc.* **36:** 349–364.

Long, J. H., Jr., and K. S. Nipper. 1996. The importance of body stiffness in undulatory propulsion. *Am. Zool.* **36:** 678–694.

McHenry, M. J., C. A. Pell, and J. H. Long, Jr. 1995. Mechanical control of swimming speed: stiffness and axial wave form in undulating fish models. *J. Exp. Biol.* **198:** 2293–2305.

Morgan, J. 1989. Analysis of beams subject to large deflections. *Aeronautical J.* **93:** 356–360.

Morgan, J., and M. G. R. Cannel. 1987. Structural analysis of tree trunks and branches: tapered cantilever beams subject to large deflections under complex loading. *Tree Physiol.* **3:** 365–374.

Niklas, K. J. 1991. The elastic moduli and mechanics of *Populus tremuloides* (Salicaceae) petioles in bending and torsion. *Am. J. Bot.* **78:** 989–996.

Niklas, K. J. 1992. *Plant Biomechanics: An Engineering Approach to Plant Form and Function.* University of Chicago Press, Chicago.

Niklas, K. J. 1998. The mechanical roles of clasping leaf sheaths: evidence from *Arundinaria tecta* (Poaceae) shoots subjected to bending and twisting forces. *Ann. Bot.* **81:** 23–34.

Prince, R. P., and D. W. Bradway. 1969. Shear stress and modulus of selected forages. *Am. Soc. Agr. Eng. Trans.* **12:** 426–428.

Putz, F. E., and N. M. Holbrook. 1991. Biomechanical studies of vines. Pp. 73–97 in *The Biology of Vines*, F. E. Putz and H. A. Mooney, eds. Cambridge University Press, New York.

Raup, D. M. 1966. Geometric analysis of shell coiling: general problems. *J. Paleontol.* **40:** 1178–1190.

Raup, D. M., and S. M. Stanley. 1971. *Principles of Paleontology.* W. H. Freeman, San Francisco.

Roark, R. J. 1943. *Formulas for Stress and Strain,* 2nd ed. McGraw-Hill, New York.

Vincent, J. 1990. *Structural Biomaterials.* Princeton University Press, Princeton, NJ.

Vogel, S. 1984. Drag and flexibility in sessile organisms. *Am. Zool.* **24:** 37–44.

Vogel, S. 1989. Drag and reconfiguration of broad leaves in high winds. *J. Exp. Bot.* **40:** 941–948.

Vogel, S. 1992. Twist-to-bend ratios and cross-sectional shapes of petioles and stems. *J. Exp. Bot.* **43:** 1527–1532.

Vogel, S. 1995. Twist-to-bend ratios of woody structures. *J. Exp. Bot.* **46:** 981–985.

Vogel, S. 1998. Convergence as an analytical tool in evaluating design. Pp. 13–20 in *Principles of Animal Design: The Optimization and Symmorphosis Debate,* E. R. Weibel, C. R. Taylor, and L. Bolis, eds. Cambridge University Press, Cambridge.

Wainwright, S. A. 1988. *Axis and Circumference: The Cylindrical Shape of Plants and Animals.* Harvard University Press, Cambridge, MA.

Wainwright, S. A., and J. R. Dillon. 1969. On the orientation of sea fans. *Biol. Bull.* **136:** 130–139.

Wainwright, S. A., W. D. Biggs, J. D. Currey, and J. M. Gosline. 1976. *Mechanical Design in Organisms.* Princeton University Press, Princeton, NJ.

Wainwright, S. A., F. Vosburgh, and J. H. Hebrank. 1978. Shark skin: function in locomotion. *Science* **202:** 747–749.

Appendix

Species (n = 57) used in the mechanospace, along with their source, diameter, flexural stiffness (EI), torsional stiffness (GJ), and the ratio EI/GJ. Species for which assumptions were made about their size and shape are marked with an asterisk. The standard deviations for EI/GJ are given in parenthesis, when available

Group	Species	Diameter (m)	EI (Nm^2)	GJ (Nm^2)	EI/GJ	Source
Crustacean antennae n = 2	*Procambarus* sp. Crayfish	0.0004	2.50E−05	6.00E−06	4.5 (3.7)	Etnier, 2001
	Panulirus argus Lobster	0.002	5.83E−03	2.04E−03	1.8 (1.3)	Etnier, 2001
Crinoid arms n = 2	*Comactinia echinoptera*	0.002	5.00E−05	1.50E−05	4.3 (3.8)	Etnier, 2001
	Florometra serratissima	0.002	3.92E−04	5.10E−05	6.6 (2.7)	Etnier, 2001
Horsetails n = 1	*Equisetum hyemale*	0.005	1.87E−02	3.83E−03	4.1 (1.8)	Etnier, 1999
Herbaceous stems n = 6	*Cucumis sativus* Cucumber	0.004	8.73E−03	1.83E−03	5.4 (1.2)	Vogel, 1992
	Helianthus annuus Sunflower	0.005	7.30E−05	5.30E−05	1.4 (0.4)	Vogel, 1992
	Lycopersicon esculenium Tomato	0.005	1.20E−02	3.46E−03	3.9 (1.1)	Vogel, 1992
	Carex acutiformis sedge	0.005	7.70E−03	2.34E−04	36.0 (11.3)	Ennos, 1993
	Tulips	0.006	2.02E−02	2.40E−03	8.3 (3.2)	Etnier and Vogel, 2000
	Narcissus pseudonarcissus Daffodil	0.007	1.19E−02	8.90E−04	13.3 (1.0)	Etnier and Vogel, 2000
Leaf petioles n = 5	*Acer rubrum* Red maple	0.001	1.94E−04	7.10E−05	2.8 (1.2)	Vogel, 1992
	Liquidambar styraciflua Sweet gum	0.002	9.84E−04	1.99E−04	5.1 (1.3)	Vogel, 1992
	Phaseolus vulgaris Green bean	0.002	6.77E−04	1.43E−04	4.9 (2.1)	Vogel, 1992
	Populus alba White popular	0.003	7.75E−05	1.50E−05	4.95	Vogel, 1992
	Populus tremuloides	0.003	1.00E−05	1.00E−06	4	Niklas, 1991
Tree roots n = 1	*Pinus taeda* Loblolly pine	0.05	1.72E+02	7.90E+01	2.3 (0.8)	Vogel, 1995
Vines n = 16	*Croton pullei* juvenile	0.01*	3.30E+00	3.04E−01	10.9	Gallenmüller *et al.*, 2001
	Cissampelos pareira	0.02*	3.63E+00	4.90E−01	7.4	Putz and Holbrook, 1991
	Cissus sicyoides	0.02*	1.15E+00	1.30E−01	8.8	Putz and Holbrook, 1991
	Forsteronia portoricesis	0.02*	1.67E+00	8.30E−01	2.0	Putz and Holbrook, 1991
	Heteropteris laurifolia	0.02*	1.07E+01	4.60E+00	2.3	Putz and Holbrook, 1991
	Hippocratea volubilis	0.02*	4.38E+00	6.80E−01	6.4	Putz and Holbrook, 1991
	Ipomoea repanda	0.02*	3.41E+00	3.10E−01	11.0	Putz and Holbrook, 1991
	Marcgravia rectiflora	0.02*	1.32E+01	2.50E−01	52.8	Putz and Holbrook, 1991
	Mikania fragilis	0.02*	1.48E+00	2.00E−01	7.4	Putz and Holbrook, 1991
	Paullinia pinnata	0.02*	4.71E+00	6.30E−01	7.5	Putz and Holbrook, 1991
	Rourea surinamensis	0.02*	6.48E+00	1.23E+00	5.3	Putz and Holbrook, 1991
	Schlegelia brachyantha	0.02*	4.34E+00	9.60E−01	4.5	Putz and Holbrook, 1991
	Securidaca virgata	0.02*	1.59E+00	3.60E−01	4.4	Putz and Holbrook, 1991
	Croton pullei mature	0.02*	4.87E+00	3.61E+00	1.4	Gallenmüller *et al.*, 2001
	Vitus rotundifolia Grape	0.046	3.08E+02	1.14E+02	2.7 (0.3)	Vogel, 1995
	Wisteria sinensis Wisteria	0.051	2.85E+02	6.70E+01	4.5 (2.1)	Vogel, 1995
Gorgonian corals n = 13	*Ellisella barbadensis*	0.004*	1.14E−01	2.16E−02	5.3	Jeyasuria and Lewis, 1987
	Eunicea calyculata	0.004*	9.07E−03	1.76E−03	5.1	Jeyasuria and Lewis, 1987
	Eunicea clavigera	0.004*	7.94E−03	2.26E−03	3.5	Jeyasuria and Lewis, 1987
	Gorgonia ventalina	0.004*	1.66E−02	1.05E−02	1.6	Jeyasuria and Lewis, 1987
	Leptogorgia virgulata	0.004*	4.47E−02	1.33E−02	3.3	Jeyasuria and Lewis, 1987
	Lophorgogia cardinalis	0.004*	6.35E−02	1.46E−02	4.3	Jeyasuria and Lewis, 1987
	Muriceopsis flavida	0.004*	8.82E−03	3.51E−03	2.5	Jeyasuria and Lewis, 1987
	Plexaura flexuosa	0.004*	1.25E−02	2.01E−03	6.2	Jeyasuria and Lewis, 1987
	Plexaurella grisea	0.004*	5.66E−02	9.54E−03	5.9	Jeyasuria and Lewis, 1987
	Pseudoplexaura crucis	0.004*	7.31E−03	2.01E−03	3.6	Jeyasuria and Lewis, 1987
	Pseudopterogorgia bipinnata	0.004*	4.17E−02	9.04E−03	4.6	Jeyasuria and Lewis, 1987
	Pterogorgia citrina	0.004*	1.95E−02	3.01E−03	6.5	Jeyasuria and Lewis, 1987
	Swiftia exserta	0.004*	8.82E−03	1.76E−03	5.0	Jeyasuria and Lewis, 1987
Tree branches n = 11	*Brunellia comocladifolia*	0.02*	2.08E+01	1.65E+00	12.6	Putz and Holbrook, 1991
	Dendropanax arboreus	0.02*	9.42E+01	2.81E+00	33.5	Putz and Holbrook, 1991
	Guarea trichilioides	0.02*	1.92E+01	1.95E+00	9.9	Putz and Holbrook, 1991
	Inga vera	0.02*	3.74E+01	5.47E+00	6.8	Putz and Holbrook, 1991
	Ocotea floribunda	0.02*	1.31E+01	4.23E+00	3.1	Putz and Holbrook, 1991
	Juniperus virginiana E. red cedar	0.04	7.44E+02	1.68E+02	4.4 (0.7)	Vogel, 1995
	Liriodendron tulipifera Tulip poplar	0.045	1.16E+03	1.30E+02	8.9 (1.4)	Vogel, 1995
	Acer rubrum Red maple	0.047	2.07E+03	2.50E+02	8.3 (0.9)	Vogel, 1995
	Phyllostachys sp. Bamboo	0.05	8.03E+03	9.50E+02	8.6 (1.3)	Vogel, 1995
	Pinus taeda Loblolly pine	0.051	2.06E+03	3.19E+02	6.1 (0.9)	Vogel, 1995
	Liquidambar styraciflua Sweet gum	0.054	2.38E+03	2.60E+02	8.9 (1.6)	Vogel, 1995